Accurate Determination and Modeling of the Dispersion of the First Hyperpolarizability of an Efficient Zwitterionic Nonlinear Optical Chromophore by Tunable Wavelength Hyper-Rayleigh Scattering

Jochen Campo,[†] Wim Wenseleers,*[,†] Etienne Goovaerts,[†] Marek Szablewski,[‡] and Graham H. Cross[‡]

Department of Physics, University of Antwerp (campus Drie Eiken), Universiteitsplein 1, B-2610 Antwerpen, Belgium, and Department of Physics, Durham University, Durham DH1 3LE, United Kingdom

Received: July 25, 2007; In Final Form: September 26, 2007

The wavelength-dependent molecular first hyperpolarizability β of the zwitterionic nonlinear optical (NLO) chromophore picolinium quinodimethane (PQDM) is determined by hyper-Rayleigh scattering (HRS) and used to test and improve theoretical β dispersion models. Experimental HRS data are obtained over a very wide fundamental wavelength range (780−1730 nm), spanning the entire range of two-photon resonance with the intramolecular charge-transfer (ICT) transition and reaching the onset of a higher energy resonance. Reliable calibration against the pure solvent (dimethylformamide, DMF, and DMF-d_7 at the longest wavelengths) was achieved over the full spectral range as a result of the high sensitivity of the HRS setup. Extremely high resonant β values are obtained (up to 4560×10^{-30} esu at 1360 nm) and also away from resonance β remains very large (1210×10^{-30} esu at 1730 nm). The two-photon resonance with the ICT band shows a pronounced red shift (∼33 nm in second-harmonic wavelength) relative to the absorption maximum. The various two-level β dispersion models available in the literature are considered, and some important improvements are introduced. Furthermore, a vibronic model including a single vibrational mode and incorporating inhomogeneous broadening is developed and contrasted to the other extreme of a continuum of vibronic lines without inhomogeneous broadening. The red shift of the β maximum can be largely explained by either an improved inhomogeneous broadening model or by vibronic coupling. However, the vibronic models are physically more realistic and lead to a better description of the observed β dispersion. In general, models with more inhomogeneous broadening result in a narrower β resonance, whereas incorporating more homogeneous broadening yields a broader resonance. Hence, the derived static electronic hyperpolarizability β_0 depends very critically on the precise modeling of the broadening mechanisms. Upper and lower bounds to the true β_0 are estimated from the two limiting vibronic models.

Introduction

Organic materials exhibiting a strong second-order nonlinear optical (NLO) response have a wide range of potential applications, such as efficient frequency doubling and fast electro-optic (EO) modulation.[1−4] At the molecular level, the parameter of importance is the first hyperpolarizability β, which is mainly measured using the hyper-Rayleigh scattering (HRS) technique[5,6] based on incoherent frequency doubling by the randomly oriented molecules in a dilute solution. However, NLO chromophores generally exhibit electronic transitions at visible to near IR frequencies. Therefore, the β value, which is very often measured at a single NIR wavelength (e.g., 1064 nm using a Nd:YAG laser system), is strongly influenced by two-photon resonance enhancement. This severely complicates the derivation of β at other wavelengths, and in particular, no reliable estimate of a static value β_0 can be made. The simple two-level model of Oudar and Chemla,[7] which is widely used in literature to extrapolate nearly resonant β values to the static limit, is neglecting line-broadening and is therefore expected to become inadequate as one enters the resonance regime. In this way, the static hyperpolarizabilities appearing in the literature can be very unreliable.[8] It is nevertheless important to obtain a dependable static value of the electronic hyperpolarizability in order to make a comparison between different molecules and with theoretical values. To reduce the resonance effect on β, several authors have performed HRS measurements at longer wavelengths such as 1300,[9] 1319,[10,11] 1340,[12] 1450,[13] 1500,[14] 1543,[15] and 1907 nm,[16,17] the latter two being accessible by Raman shifting the Nd:YAG output. Moreover, by measuring β values at several (second-harmonic, SH) wavelengths in the intramolecular charge-transfer (ICT) band of the NLO molecule, the resonance effect on β can be observed experimentally, as was demonstrated in pioneering papers by Wang and co-workers.[18−21] In the mentioned studies however, the distinction between different possible β dispersion models is severely hampered by the low signal-to-noise (S/N) ratio of the experimental results, which was attributed to intensity fluctuations of the incident laser pulses and the noise of the detection unit.[20]

In this work, a very extensive wavelength-dependent HRS study is performed. Because we make use of a very stable continuously tunable laser system with kHz repetition rate and sensitive parallel detection (enabling reliable calibration against the pure solvent over the entire wavelength range), a very detailed experimental data set with excellent S/N ratio is

* To whom correspondence should be addressed. E-mail: Wim.Wenseleers@ua.ac.be.
[†] University of Antwerp.
[‡] Durham University.

10.1021/jp0758824 CCC: $40.75
Published on Web 12/12/2007

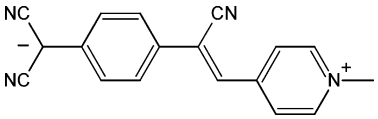

Figure 1. Chemical structure of the picolinium quinodimethane (PQDM) chromophore.

obtained to which the currently available two-level β dispersion models can be put to the test. For this study, we chose the efficient zwitterionic NLO chromophore picolinium quinodimethane[22] (PQDM, see Figure 1).

In general, derivatives of 7,7,8,8-tetracyanoquinodimethane (TCNQ)[23] allow very large dipole moments μ to be successfully combined with large first hyperpolarizabilities in one conjugated system and are therefore very interesting toward applications in poled polymer films, where the scalar product $\mu\beta$ represents the main figure of merit. Indeed, the ground state of these chromophores has a strongly charge-separated (zwitterionic) character because it is stabilized by a gain in aromaticity of the conjugated chain. This has led to very high $\mu\beta$ values,[24] which was interpreted in terms of the bond-length alternation (BLA) model.[25,26] For example, DEMI was reported[24] to have a $\mu\beta_0$ value of 9500×10^{-48} esu. PQDM however has a slightly longer conjugated chain compared to DEMI, including a second aromatic ring which further stabilizes the zwitterionic state and places it further to the right in the BLA diagram.[25,26] Indeed, a very large β value of 1865×10^{-30} esu was obtained for PQDM (about twice as large as for DEMI) by HRS at a fundamental wavelength of 1.07 μm, and it could be doped into a polymer leading to a high EO coefficient r_{33}.[27] Furthermore, it was found that the chromophore could be functionalized without affecting its favorable NLO properties,[27] opening new possibilities for improving solubility, covalent binding to polymers, and cross-linking. Indeed, polymer films with a high loading of PQDM chromophores could be achieved and improved, and stable EO coefficients were experimentally demonstrated.[28]

Hence, the wavelength-dependent HRS data for the very promising and well characterized system PQDM presented here form a relevant and critical test for the different possible β dispersion models. Because the SH wavelength is tuned through the ICT band of PQDM, the undamped two-level model[7] cannot be used, and line-broadening mechanisms will need to be introduced. First of all, one can consider homogeneous broadening by introducing an ad hoc damping parameter into the expressions,[29] and second, inhomogeneous broadening[30,31] can be included by using a convolution expression with an inhomogeneous distribution. In a next step, the vibrational structure of the absorption band has to be incorporated in the model. A lot of work has been previously performed on a theoretical description of vibronic effects on the first hyperpolarizability,[32−40] as well as on the explicit calculation of solvent effects.[41,42] However, here we mainly aim to come to a directly applicable model using only readily available experimental parameters. In this context it is worth mentioning the progress already made in this direction by Kelley,[43] in developing a vibronic model based on linear absorption. In addition to some important improvements of the existing models, we propose a new simple vibronic model taking into account coupling to a single normal mode and including inhomogeneous broadening.

Experimental Methods

The wavelength-dependent hyper-Rayleigh scattering (HRS) measurements are performed using a laser system based on an optical parametric amplifier (Spectra-Physics OPA-800CP) pumped by a Ti:sapphire regenerative amplifier (Spectra-Physics Spitfire) seeded by a mode-locked Ti:sapphire laser (Spectra-Physics Tsunami). The output of the OPA (repetition rate: 1.5 kHz, pulse width: 2 ps, pulse energy at the sample: $\sim$20 μJ from 1072 to 1600 nm, $\sim$6 μJ below 1072 nm and $\sim$13 μJ above 1600 nm) is focused onto the sample with cylindrical lenses to achieve a sufficiently high intensity while avoiding higher-order effects, and the HRS light is collected at a right angle and detected using a spectrograph with an intensified charge coupled device (Stanford Computer Optics 4 Quik E) with red-sensitive photocathode. The intensified CCD yields single-photon sensitive, nanosecond-gated, parallel registration of a $\sim$23 nm spectral region around the second-harmonic (SH) wavelength, which shortens the measurement time and enables correction for any multiphoton fluorescence (MPF) background present.[44,45] For the PQDM chromophore, MPF was observed and needed to be subtracted in the measurements with fundamental wavelength shorter than 830 nm and longer than 1150 nm. The former can originate from trace impurities or from direct fluorescence from the higher-energy excited state, which is populated by doubly resonant two-photon absorption (TPA). For a fundamental wavelength of 1550 nm, the MPF integrated over the $\sim$6 nm central region of the registered spectral range was up to 3.5 times stronger than the HRS signal. The HRS measurements are carried out on a 1 cm path length fused silica cell containing a dilute solution of picolinium quinodimethane (PQDM) in dimethylformamide (DMF), and they could be calibrated against the pure solvent over the entire wavelength range, thanks to the high sensitivity of the experimental setup. In the present work, for DMF, the effective β value of 0.70×10^{-30} esu was obtained from external reference to chloroform at 1072 nm for which the EFISHG value of 0.49×10^{-30} esu was adopted,[46] assuming spherical Lorentz−Lorenz local field factors for both solvents as described previously.[45]

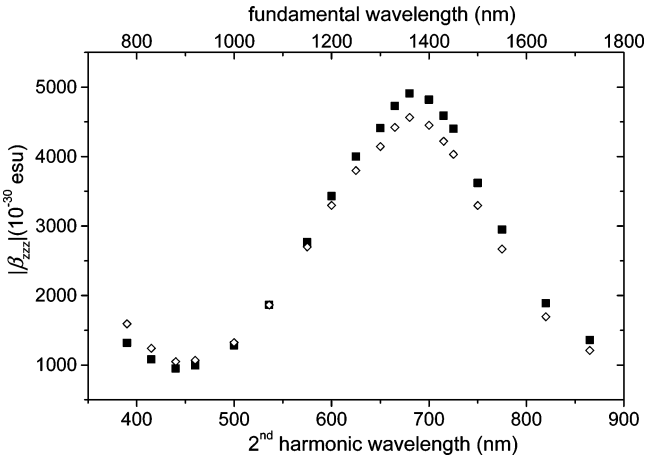

Figure 2. Wavelength-dependent HRS data of PQDM in DMF (in DMF-d_7 at the SH wavelengths of 820 and 865 nm): uncorrected (solid squares) and corrected (hollow diamonds) for the β dispersion of the pure solvent.

Although the β dispersion of pure DMF is expected to be very low, it may become significant over the broad wavelength range of the present HRS measurements. This effect was taken into account using the undamped two-level model (TLM) with $\lambda_{eg} \approx 200$ nm, which is the λ_{max} of the lowest energy UV transition as we determined from the absorption spectrum of vapor-phase DMF. The effect of this correction on the actual experimental data for PQDM is quite limited, as shown in Figure 2.

The concentrations used (10^{-6} to 10^{-5} M) were chosen in order to keep the absorption of the SH wavelength well below

10%, so that only small corrections had to be performed to compensate for this effect. The β values are obtained within the assumption of only one significant tensor component β_{zzz}, as discussed at length previously.[45] HRS measurements were successfully performed over the extensive wavelength range from 780 to 1730 nm. The accessible spectral region is limited at the short wavelength side by the absorption-induced decomposition of the PQDM chromophore and at the long wavelength side ultimately by the decreasing sensitivity of the detection system but also by the infrared absorption of the solvent. Transparency in the whole range could be obtained in the solvent deuterated DMF (DMF-d_7, ACROS, 99.5 atom % D), which is electronically equivalent. Indeed, Kaatz et al.[47] have demonstrated that β values for hydrogenated and deuterated solvents are equal to within an experimental error of 5%. For the β values obtained in the present work, the experimental error (not including the systematic error of the reference standard value) is estimated to be about $\pm$3%. The comparison of experiments in DMF with those in DMF-d_7 also allowed us to exclude possible thermal-lensing effects and/or vibrational contributions to β associated with the weak solvent absorption bands.

Theory

Several two-level models (TLM) to describe the dispersion of the molecular first hyperpolarizability β have been published.[7,29−31,48] In this section we briefly review these models, and some essential improvements are introduced. In a first, very rough approximation, there is the simple undamped TLM of Oudar and Chemla,[7] which is completely neglecting line-broadening of the transition. This model can be improved by including homogeneous damping in the β expressions[29,48] or by considering inhomogeneous broadening.[30,31,48] As a next step, the vibrational structure of the excited-state can be taken into account using a purely homogeneous vibronic-like model (e.g., the model of Kelley based on the linear absorption spectrum),[43] and finally, a new simple vibronic dispersion model is proposed, coupling to a single normal mode and including inhomogeneous broadening. Note that, because we are only concerned with the description of the wavelength dependence, the factors coming from orientational averaging will not be included explicitly in the upcoming β expressions. These factors could also be incorporated in the equations, but for simplicity, we will take β to represent the derived β_{zzz} component (in both left- and right-hand sides of the expressions). In addition, throughout the theoretical discussion below, we will only consider the frequency component of β associated with frequency doubling, which is generally written as $\beta(-2\omega;\omega,\omega)$, but will be abbreviated here as $\beta^{\mathrm{SHG}}(\omega)$ (with ω = fundamental frequency) to avoid confusion between the frequency arguments and any additional parameters used as arguments in the models.

Undamped Two-Level Model. A strongly simplified model to describe the β dispersion is the TLM of Oudar and Chemla.[7] They made the assumption that only one excited state (the ICT state, generally the lowest energy transition observed in the absorption spectrum) yields the dominant contribution to β, leading to the reduction of the sum-over-states (SOS) expression[29] to the following form:[1,7,49]

$$\beta^{\mathrm{SHG}}(\omega,\omega_{\mathrm{eg}}) = \beta_0 \frac{\omega_{\mathrm{eg}}^4}{(\omega_{\mathrm{eg}}^2 - \omega^2)(\omega_{\mathrm{eg}}^2 - 4\omega^2)} \qquad (1)$$

in which $\beta_0 = 3e^2 f_{\mathrm{osc}} \Delta\mu / 2\hbar m \omega_{\mathrm{eg}}^3$ is the static first hyperpolarizability, ω_{eg} corresponds to the energy of the electronic transition, ω is the laser frequency, f_{osc} is the oscillator strength of the transition, and $\Delta\mu$ is the difference between the ground and excited-state dipole moments. Due to the total neglect of line-broadening mechanisms, this expression diverges when the fundamental laser wavelength or its second harmonic (SH) equals the transition wavelength of the molecule and is expected to be valid only far from resonance. Nevertheless, thanks to its simplicity this is by far the most popular model, used almost universally (yet inappropriately) to extrapolate resonant hyperpolarizabilities to the static limit, usually taking ω_{eg} to be the absorption maximum.

Homogeneously Damped Two-Level Model. The easiest way to incorporate a finite line-width for the optical transition is the phenomenological approach originally developed by Orr and Ward,[29] introducing an ad hoc damping parameter γ into the denominators of the terms in the SOS expression, leading to the following expression for β:[48]

$$\beta^{\mathrm{SHG}}(\omega,\omega_{\mathrm{eg}},\gamma) = \beta_0 F(\omega,\omega_{\mathrm{eg}},\gamma) \qquad (2)$$

with

$$F(\omega,\omega_{\mathrm{eg}},\gamma) = \frac{\omega_{\mathrm{eg}}^2}{3}\left[\frac{1}{(\omega_{\mathrm{eg}} + i\gamma + 2\omega)(\omega_{\mathrm{eg}} + i\gamma + \omega)} + \frac{1}{(\omega_{\mathrm{eg}} - i\gamma - 2\omega)(\omega_{\mathrm{eg}} - i\gamma - \omega)} + \frac{1}{(\omega_{\mathrm{eg}} + i\gamma + \omega)(\omega_{\mathrm{eg}} - i\gamma - \omega)}\right]$$

Several approximations to this homogeneously broadened model have been made such as neglecting or changing the sign of the damping in the nondivergent terms,[48,50] leading to simpler forms generally deviating from eq 2 by only a few percent. However, these deviations increase with increasing damping and with decreasing ω_{eg}.

Inhomogeneously Broadened Two-Level Model. For a molecule in the condensed phase, it is physically unrealistic to attribute the full line width of the excited-state to damping (electronic pure dephasing and lifetime broadening) only. In fact, inhomogeneous line-broadening (e.g., solvent-induced frequency shift) is likely to be far more important. It is therefore useful to consider another limiting case of a line shape dominated completely by inhomogeneous broadening. We make use of the fact that the absorption spectrum Abs(ω) contains all of the necessary information about the distribution function

$$\mathrm{Abs}(\omega'_{\mathrm{eg}}) \propto f_{\mathrm{osc}}(\omega'_{\mathrm{eg}})\, N(\omega'_{\mathrm{eg}}) \propto \omega'_{\mathrm{eg}} |\mu_{\mathrm{eg}}|^2 N(\omega'_{\mathrm{eg}}) \qquad (3)$$

with $f_{\mathrm{osc}}(\omega'_{\mathrm{eg}}) \propto \omega'_{\mathrm{eg}} |\mu_{\mathrm{eg}}|^2$ the oscillator strength, μ_{eg} the transition dipole moment, and $N(\omega)$ the normalized distribution of the transition frequencies of the molecules. Now, with each molecule corresponds a homogeneously damped β, each with a different ω_{eg} in the inhomogeneous distribution. For coherent second-harmonic generation (SHG) processes (such as electric field induced second-harmonic generation (EFISHG)), the following convolution is obtained:

$$\beta_{\mathrm{coh}}^{\mathrm{SHG}}(\omega) = \int N(\omega'_{\mathrm{eg}})\,\beta(\omega,\omega'_{\mathrm{eg}},\gamma)\,\mathrm{d}\omega'_{\mathrm{eg}}$$
$$\propto \int \frac{\mathrm{Abs}(\omega'_{\mathrm{eg}})}{\omega'_{\mathrm{eg}}|\mu_{\mathrm{eg}}|^2}\frac{\Delta\mu|\mu_{\mathrm{eg}}|^2}{\omega'^{\,2}_{\mathrm{eg}}}F(\omega,\omega'_{\mathrm{eg}},\gamma)\,\mathrm{d}\omega'_{\mathrm{eg}}$$
$$\propto \int \frac{\mathrm{Abs}(\omega'_{\mathrm{eg}})}{\omega'^{\,3}_{\mathrm{eg}}}\Delta\mu F(\omega,\omega'_{\mathrm{eg}},\gamma)\,\mathrm{d}\omega'_{\mathrm{eg}} \quad (4)$$

where we used expression 3 to insert the absorption spectrum and expression 2 for the homogeneously damped hyperpolarizability (with $\beta_0(\omega'_{\mathrm{eg}}) \propto \Delta\mu f_{\mathrm{osc}}/\omega'^{\,3}_{\mathrm{eg}} \propto \Delta\mu|\mu_{eg}|^2/\omega'^{\,2}_{\mathrm{eg}}$). Now, if we assume $\Delta\mu$ to be constant throughout the inhomogeneous distribution of molecules, eq 4 can be used to calculate the dispersion of β_{coh}. Either the experimental absorption spectrum itself (over the frequency range of the ICT band) or a Gaussian fit can be inserted in eq 4. The homogeneous damping parameter γ is fixed arbitrarily at a very small value ($\sim$40 cm^{-1}), serving here only as a small but finite constant to avoid divergence in the numerical calculation. Note that eq 4 is different from the expression mentioned explicitly in ref 48 (but already used in earlier work[30,31]), because there the factor of ω occurring between the transition dipole and the oscillator strength, as needed to relate the β dispersion with experimental absorption, is not taken into account. This results in an extra factor ω_{eg} in the denominator of the convolution (eq 4) compared to the Berkovic expression.[48] This seemingly subtle change results in an increase of the (already quite significant) red shift between the two-photon resonance peak position and the linear absorption maximum, which will turn out to be important in the modeling of the experimental data (see the Results and Discussion). Another important consideration is that the equation derived for coherent SHG cannot be applied to the incoherent process of HRS (as was done inappropriately in ref 51). Instead of the coherent sum in eq 4, the hyperpolarizabilities of the different molecules now have to be summed incoherently, to obtain $\beta_{\mathrm{incoh}}^{\mathrm{SHG}}$ (i.e., the β derived from HRS measurements):

$$(\beta_{\mathrm{incoh}}^{\mathrm{SHG}}(\omega))^2 = \int N(\omega'_{\mathrm{eg}})\,||\beta(\omega,\omega'_{\mathrm{eg}},\gamma)||^2\,\mathrm{d}\omega'_{\mathrm{eg}}$$
$$\propto \int \frac{\mathrm{Abs}(\omega'_{\mathrm{eg}})}{\omega'_{\mathrm{eg}}|\mu_{\mathrm{eg}}|^2}\left(\frac{\Delta\mu|\mu_{\mathrm{eg}}|^2}{\omega'^{\,2}_{\mathrm{eg}}}\right)^2||F(\omega,\omega'_{\mathrm{eg}},\gamma)||^2\,\mathrm{d}\omega'_{\mathrm{eg}}$$
$$\propto \int \frac{\mathrm{Abs}(\omega'_{\mathrm{eg}})}{\omega'^{\,6}_{\mathrm{eg}}}\Delta\mu^2 f_{\mathrm{osc}}||F(\omega,\omega'_{\mathrm{eg}},\gamma)||^2\,\mathrm{d}\omega'_{\mathrm{eg}} \quad (5)$$

where we made use of the same identities as in the derivation of eq 4. As already mentioned above, the orientational averaging factors are not included in eq 5, as we are focusing on the description of the wavelength dependence and take $\beta_{\mathrm{incoh}}^{\mathrm{SHG}}$ to represent the derived β_{zzz} component. Because now the oscillator strength f_{osc} is not cancelled out in the equation (as was the case in eq 4), we are forced to make the somewhat arbitrary assumption that $\Delta\mu^2 f_{\mathrm{osc}}$ is constant over the distribution (an alternative would be to consider $\Delta\mu^2|\mu_{\mathrm{eg}}|^2$ fixed). It appears that keeping track of the appropriate ω factors has an even stronger effect in eq 5 than in eq 4. For the case of a Gaussian absorption band ($N(\omega'_{\mathrm{eg}}) \propto e^{-(\omega'_{\mathrm{eg}}-\omega_{\mathrm{eg}})^2/G^2}$; thus, $G \approx 1.20 \times$ half-width-at-half-maximum, HWHM) and taking only the two-photon resonant term of $F(\omega,\omega_{\mathrm{eg}},\gamma)$ into account with infinitely small damping, the red shift $\Delta\omega$ predicted by eq 5 is found to follow the relationship:

$$\frac{\Delta\omega}{\omega_{\mathrm{eg}}} := \frac{\omega_{\mathrm{eg}} - 2\omega_{\mathrm{2PR}}}{\omega_{\mathrm{eg}}} \approx \frac{1}{2} - \frac{1}{2}\sqrt{1 - 8\frac{G^2}{\omega_{\mathrm{eg}}^{\,2}}} \quad (6)$$

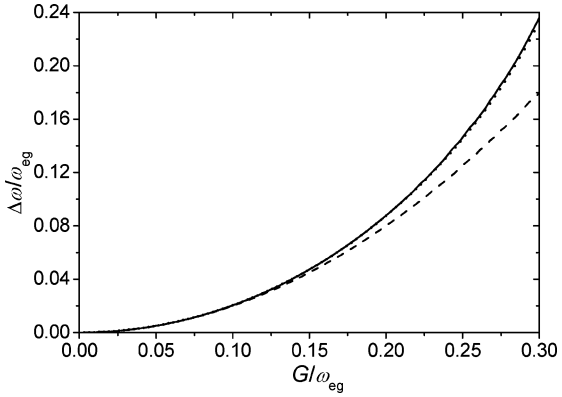

Figure 3. Relative red shift $\Delta\omega/\omega_{\mathrm{eg}}$ between the position of the two-photon resonance maximum of β_{HRS} and the absorption maximum within the inhomogeneously broadenened two-level model (eq 5) as a function of the relative Gaussian width G/ω_{eg} (dotted line: numerically calculated from the full expression eq 5 [γ = 40 cm^{-1}], nearly coincident with the solid line: analytical result eq 6, and dashed line: quadratic approximation).

where ω_{2PR} is the position of the two-photon resonance (2PR) maximum. For realistic Gaussian widths G (for most dyes $G/\omega_{\mathrm{eg}} \lesssim 0.15$), eq 6 can be accurately approximated by a quadratic dependence on the bandwidth ($\Delta\omega/\omega_{\mathrm{eg}} \approx 2G^2/\omega_{\mathrm{eg}}^{\,2}$, see Figure 3).

Purely Homogeneous Vibronic-Like Model. It should be realized that the above-mentioned inhomogeneously broadened model does not give a physically realistic description either, since for an organic conjugated chromophore the overall width of the absorption band will be most likely dominated by the vibronic structure of the excited-state rather than inhomogeneous effects. Indeed, most organic chromophores display asymmetric absorption bands which are a telltale sign of the underlying vibronic sidebands; many chromophores even show a clearly resolved vibronic structure. The importance of the incorporation of vibronic coupling in the analysis of wavelength dependent β measurements has been stressed before.[18,20,41,50,52,55] In a first attempt to include vibrational levels into a simple β dispersion model, we can consider a limiting case of many vibrational modes with small homogeneous width, according to which the broad absorption band can be described as a weighed sum of very many narrow vibronic lines. In this case, β becomes a coherent sum over all vibronic transitions (only slightly homogeneously broadened) of the corresponding hyperpolarizabilities:

$$\beta^{\mathrm{SHG}}(\omega,\gamma) = \sum_n \beta_0^n F(\omega,\omega_n,\gamma) \quad (7)$$

For each term, we can apply the relation for the homogeneously damped TLM $\beta_0^n \propto \Delta\mu\, f_{\mathrm{osc}}^n/\omega_n^3$. The absorption spectrum $\mathrm{Abs}(\omega) \propto \sum_n f_{\mathrm{osc}}^n L(\omega - \omega_n,\gamma)$ is the corresponding sum of Lorentzian bands $L(\omega - \omega_n,\gamma)$, with γ the HWHM, which is much smaller than the absorption bandwidth. As we consider the limiting case of a large number of closely spaced (not necessarily equidistant) transitions, the summation weighed by f_{osc}^n can be replaced by an integration over the absorption spectrum, which leads to the following expression for this purely homogeneous vibronic-like model:

$$\beta^{\mathrm{SHG}}(\omega,\gamma) \propto \Delta\mu \int \frac{\mathrm{Abs}(\omega'_{\mathrm{eg}})}{\omega'^{\,3}_{\mathrm{eg}}}F(\omega,\omega'_{\mathrm{eg}},\gamma)\,\mathrm{d}\omega'_{\mathrm{eg}} \quad (8)$$

with ω'_{eg} running over the ICT absorption band and γ very small

($\sim$40 cm^{-1}). Note that the dipole moment difference $\Delta\mu$ between the ground and excited state is assumed to be equal for all vibrational sublevels.

A similar approach in which information on both homogeneous broadening and vibrational structure of the excited-state is included based on the experimental absorption spectrum has been proposed by Kelley.[43] She showed that, within the usual assumptions of a TLM, the β dispersion can be approximated by[43]

$$\beta^{\mathrm{SHG}}(\omega) = \frac{\Delta\mu}{\hbar^2(\omega_{\mathrm{eg}} - \omega)}\left(\frac{\mu_{\mathrm{eg}}{}^2(2\omega_{\mathrm{eg}} + \omega)}{(\omega_{\mathrm{eg}} + \omega)(\omega_{\mathrm{eg}} + 2\omega)} + \chi(2\omega)\right) \tag{9}$$

where $\Delta\mu$ is the difference between the ground and excited-state dipole moments, ω_{eg} is an average electronic transition frequency (e.g., the weighed average of the ICT band), μ_{eg} is the transition dipole moment, and χ is the complex susceptibility. Both μ_{eg} and the imaginary part of χ can be directly calculated from the linear absorption spectrum, and the real part of χ is then obtained through a Kramers−Kronig transformation of the latter. In this way, the absorption spectrum itself, which is incorporating all of the factors responsible for its exact shape within the assumptions of the model, is directly included in the calculation of the hyperpolarizability dispersion. However, to reach the elegant relationship between the two-photon resonant part of the β expression and the linear susceptibility, Kelley had to introduce two types of approximations which turn out to influence the β dispersion curves significantly. First, the damping constants are neglected in all factors except the two-photon resonant one, and second (more important), the vibrational frequencies in these factors are omitted, using an average electronic transition frequency instead. However, these simplifications are only required in Kelley's approach to directly link the hyperpolarizability with the linear susceptibility,[43] but as demonstrated by eq 8, they are not needed to come to a useful expression. The absorption-based model of Kelley is indeed reproduced if the same two approximations are implemented in our full expression 8.

To improve on this purely homogeneous approach starting from the linear absorption, Kelley et al.[41,53,54] have developed a more advanced vibronic β dispersion model, incorporating both homogeneous and inhomogeneous broadening as well as coupling with the vibrational modes of the molecule. In this vibronic model, the excited-state parameters which are needed to describe the frequency dependence of β are extracted from simultaneous modeling of the linear absorption and resonance (hyper-)Raman data using time-dependent wave packet propagation methods. With this procedure, reasonable agreement was obtained with the (albeit very noisy) experimental HRS data for two thiophene-based CT chromophores,[20] and very recently the above-mentioned model was, apart from hyper-Rayleigh, also fitted to hyper-Raman data for DANS and a water-soluble analog.[55] However, because this more detailed model requires a lot of additional parameters that have to be determined from extensive resonant Raman and hyper-Raman measurements, it will not be applied in this work. Instead a model including only one vibrational mode will be considered as a useful limiting case.

Single-Mode Vibronic Model. Here we combine the simplest possible vibronic model, namely that of an electronic transition coupled linearly to just one normal mode, with inhomogeneous broadening of the electronic transition. As the main vibrational modes coupling to the intramolecular charge-transfer transition of organic chromophores are typically CC-stretching vibrations with frequencies >1000 cm^{-1}, it is reasonable to assume that only the lowest vibrational level of the electronic ground state is populated at room temperature. In this case, the relative intensities of the absorption bands at $\hbar\omega_n = E_{\mathrm{eg}} + n\hbar\omega_{\mathrm{vib}}$, corresponding to a transition to the nth vibrational level of the excited state, are given by[56]

$$W_n(S) = \frac{S^n e^{-S}}{n!} \tag{10}$$

with S representing the coupling strength. For the derivation of this expression, the vibration is treated as a harmonic oscillator with the same frequency in the ground and the excited state. The relative intensity $W_n(S)$ is directly proportional to the transition dipole squared $\mu_{\mathrm{eg}}{}^2$,[56] so that absorption $\propto f_{\mathrm{osc}} \propto \omega\ \mu_{\mathrm{eg}}{}^2$ is described by $\omega_n\ W_n(S)$. In this way, S can be obtained by fitting the experimental absorption band to a series of Gaussians with weights $\omega_n\ W_n(S)$

$$\mathrm{Abs}(\omega) \propto \sum_n \omega_n W_n(S)\ \mathrm{e}^{-(\omega - \omega_n)^2/G^2} \tag{11}$$

with G the Gaussian width of the individual (equidistant) vibrational bands. So, absorption is described by a series of inhomogeneously broadened vibrational lines. Accordingly, the hyperpolarizability can be written as an (inhomogeneous) convolution of a coherent sum of weakly homogeneously damped β systems

$$\begin{aligned}(\beta^{\mathrm{SHG}}_{\mathrm{incoh}}(\omega))^2 &\propto \int \mathrm{e}^{-x^2/G^2} \left|\left|\sum_n \beta_0^n F(\omega, \omega_n + x, \gamma)\right|\right|^2 \mathrm{d}x \\ &\propto \int \mathrm{e}^{-x^2/G^2} \left|\left|\sum_n \frac{\omega_n W_n(S)}{(\omega_n + x)^3} F(\omega, \omega_n + x, \gamma)\right|\right|^2 \mathrm{d}x\end{aligned} \tag{12}$$

where we used again the proportionality $\beta_0^n \propto \Delta\mu\ f^n_{\mathrm{osc}}/\omega_n{}^3$ (with $f^n_{\mathrm{osc}} \propto \omega_n W_n(S)$). Also here the dipole moment difference $\Delta\mu$ is assumed to be the same for all vibrational levels. To approximate the undamped limit the homogeneous width γ can again be set to a very small value ($\sim$40 cm^{-1}), only to avoid the divergence of the integrand at resonance. The two vibronic models introduced here (eqs 8 and 12) are the physically most realistic ones considered up to this point, because they incorporate the vibrational coupling as the main broadening mechanism. They form two limiting cases, from a continuum of vibrational modes, without inhomogeneous effects, to a single mode combined with a maximal amount of inhomogeneous broadening.

Results and Discussion

The experimental wavelength-dependent hyper-Rayleigh scattering (HRS) data of the PQDM chromophore are shown in Figure 4 together with the absorption spectrum. The β values are plotted as a function of the second-harmonic (SH) wavelength for direct comparison of the two-photon resonance with the absorption band.

Extremely high resonant β values are obtained (up to 4560 $\times$ 10^{-30} esu at 1360 nm) and also far from resonance β remains very large (1210 $\times$ 10^{-30} esu at 1730 nm). The data clearly show a very pronounced two-photon resonance with the ICT band at λ_{max} = 647 nm and, furthermore, reveals the onset of a second resonance at short wavelengths. This resonance can

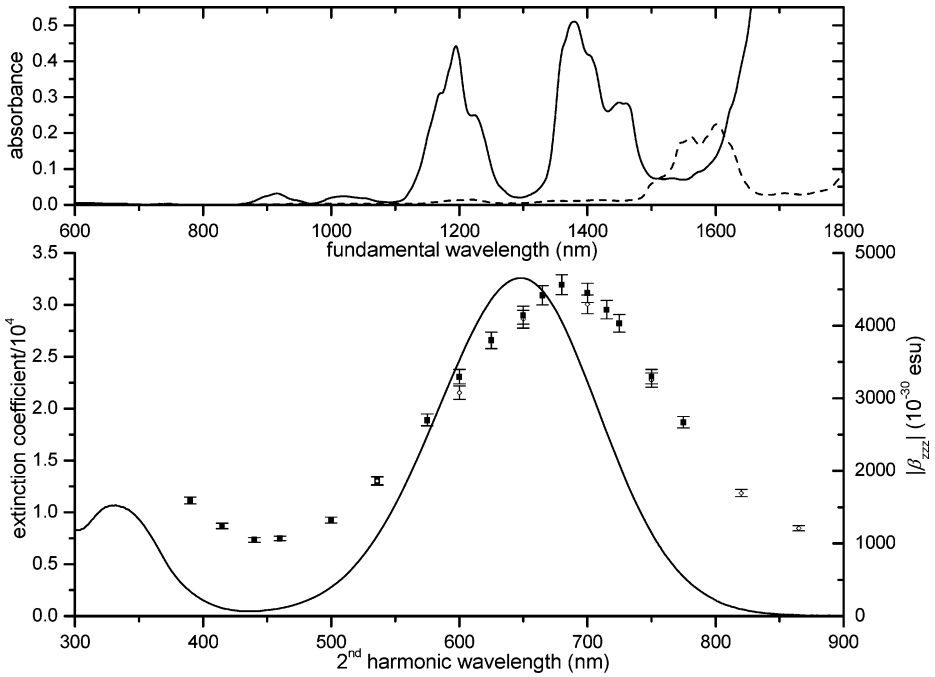

Figure 4. Below: the experimental HRS data of PQDM in DMF (solid squares) and DMF-d_7 (hollow diamonds) corrected for the β dispersion of the pure solvent, plotted at the SH wavelength together with the absorption spectrum (solid line). The upper figure shows the linear absorption spectra of the pure solvents DMF (solid line) and DMF-d_7 (dashed line), at the corresponding fundamental wavelength.

be attributed either to one-photon resonance with the same ICT transition or to two-photon resonance with the higher-energy electronic transition observed in the absorption spectrum, as this coincidentally lies at almost exactly twice the energy of the lowest energy ICT band. In Figure 4, it is also clear that the maximum of β is strongly red-shifted compared to the absorption maximum (~33 nm in SH wavelength).

Indications for spectral shifts (both red[19,20,30,57,58] and blue[18]) have been obtained previously, and it is a challenge to explain this effect theoretically. A very pragmatic approach to account for the observed blue shift has been to describe β by a two-photon resonance with one vibrational level of the excited-state instead of with the purely electronic transition, simply resulting in an ad hoc shift of the homogeneously damped TLM.[18] We also observed a large red shift for an organometallic complex[58] which was however not analyzed because of the small amount of available experimental data and because it concerns an electronically very complex system.

Also shown in Figure 4 are the absorption spectra of the pure solvents dimethylformamide (DMF) and deuterated DMF (DMF-d_7). DMF exhibits two weak absorption bands at about 1195 and 1380 nm originating from vibrational overtones and combination peaks involving the C−H stretching vibrations. A priori, it was not clear whether the measurements in these regions would be reliable because absorption of the fundamental wavelength can possibly lead to unwanted thermal lensing effects, as well as vibrational contributions to β of DMF. Therefore, these measurements were checked in DMF-d_7 and, as can be seen in Figure 4, excellent agreement is obtained with the hydrogenated DMF results. This observation, together with the absence of any peculiarities in the evolution of the β values in the proximity of the DMF absorption bands, demonstrates that the present HRS setup is not subject to significant thermal effects or vibrational influences and is therefore yielding dependable β values. Deuterated DMF also allows measurements at wavelengths longer than 1600 nm which is of great value in modeling the β dispersion and estimating the off-resonant β.

The HRS measurements were calibrated against the pure solvent over the entire wavelength range. Because of the very low β dispersion of the solvent, this procedure yields a good consistency between the molecular first hyperpolarizabilities β at different wavelengths, in contrast to previously reported wavelength-dependent HRS results,[18−21] where generally two different reference standards (*para*-nitroaniline (*p*NA) and Disperse Red 1 (DR1)) were needed for external calibration in different wavelength regions because the pure solvent signals[59] (as well as the *p*NA signals)[18] were too weak to be detected at longer wavelengths. This large set of experimental β values can now be used to confront the various dispersion models.

Undamped Two-Level Model. As expected, the simple two-level model of Oudar and Chemla[7] (TLM, see theoretical section, eq 1) based on the least resonant β value is not at all suitable to describe the more resonant values (see Figure 5a).

Homogeneously Damped Two-Level Model. The homogeneously damped TLM (eq 2) is found to give a very poor description of the β dispersion (see Figure 5a, where both β_0 and γ are optimized to fit the data), the overestimation at long wavelengths being in agreement with earlier observations.[30,59] The accurate modeling of the long wavelength tail of the dispersion is evidently very important in deriving the static limit of β. Although the position of the two-photon resonance peak in this homogeneous model can differ slightly from two times λ_{eg} (a blue shift, turning into a red shift for very large γ), this model is in no way able to predict the experimentally observed red shift for realistic linewidths. The value obtained for γ (1916 cm^{-1}) is somewhat larger than the HWHM of the ICT band of PQDM (~1800 cm^{-1}), the shape of which is not modeled correctly at all, and the corresponding blue shift is ~1 nm in SH wavelength. The discrepancy with the experimental results is however understandable, because it is physically unrealistic to consider damping as the main broadening mechanism for the excited state.

Inhomogeneously Broadened Two-Level Model. The inhomogeneous model (eq 5, see Figure 5a, where the amplitude was serving as the only fit parameter and a nearly perfect multi-

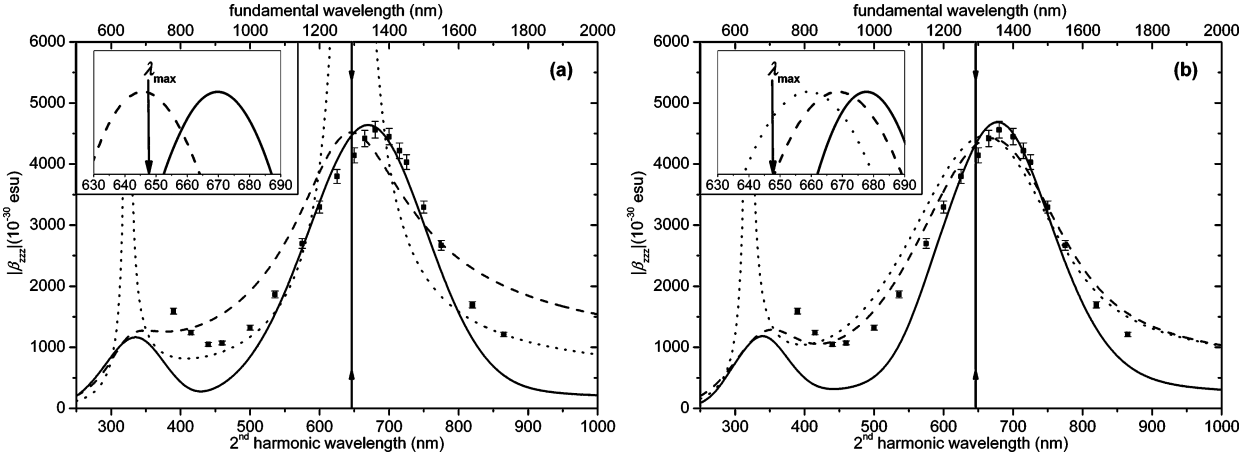

Figure 5. Two-level models (TLM) fitted to the experimental HRS data in DMF (squares, in DMF-d_7 at the SH wavelengths of 820 and 865 nm), corrected for the β dispersion of the pure solvent. Only the experimental data at SH wavelengths ≥600 nm, i.e., the two-photon resonant β values, were taken into account in the fitting procedure. (a) Dotted line: undamped TLM[7] based on the least resonant β value, dashed line: homogeneously broadened TLM,[29] solid line: inhomogeneously broadened TLM, (b) dashed line: purely homogeneous vibronic-like model, dotted line: linear absorption-based model of Kelley,[43] solid line: single-mode vibronic model. In the insets, the region of the two-photon resonance (normalized) is magnified in order to clearly show the shifts predicted by the different models.

Gaussian fit of the experimental ICT absorption band was used), shows quite a large red shift for PQDM (∼23 nm in SH wavelength compared to λ_{max}) but still too small to match the experimental data. It should be noted that if the approach of Berkovic[48] were used (ignoring a factor ω between $|\mu_{eg}|^2$ and absorption, and setting μ_{eg} constant, see theoretical section) a two times smaller red shift would have been obtained (nevertheless, this shift appears to be large enough to describe the NLO dispersion of a 4-dimethylamino-4′-nitrostilbene (DANS) side chain poled polymer[31]). The expression for the coherent case from refs 48 and 51 would also result in a much smaller red shift of about 16 nm in SH wavelength. Using eq 5, the overall shape of the two-photon resonance is already much better described, and the increase of the red shift with larger bandwidth (see theoretical section) is in line with the large red shift that we observed for an organometallic complex,[58] which was exhibiting an even broader charge-transfer band. Note that, although PQDM exhibits a very broad and low-energy ICT band, the quadratic approximation of the red shift as a function of the bandwidth is still valid (HWHM ≈ 1800 cm^{-1} combined with ω_{eg} = 15456 cm^{-1} leads to $G/\omega_{eg} \approx 0.14$).

Purely Homogeneous Vibronic-Like Model. The width of the absorption band of PQDM is expected to originate from the (unresolved) vibronic structure rather than inhomogeneous broadening. Therefore, we can consider the purely homogeneous vibronic-like model (eq 8), in which the absorption band is described by a weighed sum of very many vibrational (Lorentzian) lines. This model, which seems physically more relevant than the previous ones, was also fitted to our HRS data for PQDM (see Figure 5b), with again the amplitude as only fit parameter. From Figure 5b, it is clear that a significant red shift is obtained (∼22 nm in SH wavelength) but unfortunately still not really sufficient to fit with the experiment, and the overall shape is closer to the experiment than in previous models. However, the tails of the resonance still appear somewhat longer in the model curve compared to the experiment. Note that less fit parameters (only the amplitude) are used here than in the homogeneously damped TLM, in which also the spectral width had been adjusted.

A similar vibronic-like model in which the β dispersion is obtained directly from the linear absorption spectrum is the initial model of Kelley[43] (eq 9), which has also been used by Wang and Tai et al.[19,21] The resulting curve for the β dispersion is also shown in Figure 5b, with $\Delta\mu$ as only fit parameter and with λ_{eg} = 638 nm (the weighed average of the absorption band, only slightly different from λ_{max} = 647 nm).[60] The optimized $\Delta\mu$ was found to be 15.9 D and for μ_{eg} a value of 10.3 D was obtained directly from the absorption band, as described in ref 43. The line shape in the absorption-based model of Kelley[43] (eq 9) is found to be very similar to that in the purely homogeneous vibronic-like model (eq 8), which can be understood from the close relationship between both models. Apparently, the additional approximations introduced by Kelley cause the red shift of the purely homogeneous vibronic-like model to decrease by a factor of ∼2 (and the one-photon resonance is now undamped). As a result, the red shift is more strongly underestimated in the approach of Kelley (only ∼ 12 nm in SH wavelength), a discrepancy which could not be recognized in previous experimental work.[19] Moreover, just as for our homogeneous vibronic-like approach (eq 8), the theoretical β dispersion is exhibiting too high tails. In the original article,[43] the Kelley model was fitted to the tunable wavelength HRS data of the push−pull molecule guaiazulenethiobarbituric acid (GATB),[18] and also for that case an overestimation of the β values in the long wavelength tail was obtained. This deviation was then interpreted as a violation of the assumptions of the two-state model, indicating that higher-energy states need to be incorporated.

Single-Mode Vibronic Model. The poor fit obtained using the model of Kelley and even from the purely homogeneous vibronic-like model shows that improvements are necessary to properly describe the line-broadening effects. Therefore, we apply the limiting case of the single-mode vibronic model including inhomogeneous broadening, as described in the theoretical section (eq 12). Making use of eq 11, a very good fit of the experimental absorption band of PQDM was obtained with six Gaussian vibronic bands (the sixth one being negligible in intensity), with ω_{vib} fixed at 1550 cm^{-1} and HWHM = 1196 cm^{-1}, λ_{00} = 672 nm, and S = 0.65 treated as fit parameters (with Lorentzian bands no acceptable fit could be obtained). The frequency ω_{vib} = 1550 cm^{-1} is taken as a representative value for the most prominent vibrational modes (C−C, C═C, and C≡N stretching vibrations) coupling to the electronic transition, as observed in resonant Raman measurements of PQDM in DMF. As shown in Figure 5b, this procedure yields a red shift of 31 nm in SH wavelength, in good agreement with

the experimental observation. This can be attributed partly to the effects of inhomogeneous broadening and partly to the vibronic structure: Indeed, less than 40% of this shift (12 nm) would result, if the same Gaussian width (1435 cm^{-1}) as obtained here for the individual vibrational lines were inserted in the inhomogeneously broadened TLM (eq 5). Thus, also the vibrational structure contributes significantly to the spectral shift of the β resonance. Although in this model the red shift is close to the experimental one, the theoretical resonance is still too narrow, just as for the inhomogeneously broadened TLM. Also the increase of β below 880 nm (440 nm SH) is not well predicted, indicating that this resonance effect is only partly due to one-photon resonance with the lowest energy charge-transfer (ICT) transition and that there is a significant contribution from the higher energy transition which is visible in the absorption spectrum, but not included in the model.

We also tried increasing γ, which caused the red shift to increase even more and the resonance to broaden resulting in a very good description of the first resonance in β using a still typical γ for molecules in solution[61] (see the Supporting Information, Figure S1b) but which was unfortunately not consistent with the relatively sharp long wavelength tail of the absorption spectrum (using Voigt-profiles instead of Gaussian bands in eq 11, see inset of Figure S1b). Even if we allow the other parameters (G, λ_{00}, S, and the overall intensity) to vary, the description of the absorption band is still not as good as was obtained with the smaller homogeneous width (40 cm^{-1}). So it appears that the homogeneous damping γ needs to be very small (in the order of 40 cm^{-1}) to be able to describe the ICT band correctly (see Figure S1a). This was also the case in ref 31, where it was found that a homogeneously damped TLM is not able to give a good description of the long-wavelength tail of the absorption spectrum for an organic dye molecule.[30,31] Hence, in spite of the good fit of the two-photon resonance of β for increased homogeneous width γ, this approach is physically unacceptable. Note that also here the increase of β below 880 nm remains insufficient compared to the experimental result.

So we find that the present simple vibronic model yields a reasonable fit of the data; the predicted red shift is in good agreement with experiment, whereas the shape of the resonance is still not perfect. Of course, also this model is based on a number of approximations that should be critically considered. The following three attempts were made in order to improve on the mentioned shortcomings of the β model: (i) The homogeneous widths of the excited-state vibrational levels were all taken to be equal up to this point, whereas the vibrational relaxation rate is expected to contribute to this width for the $n > 0$ levels, and increasingly for higher levels. Therefore, we introduced a homogeneous width $\gamma_n = \gamma_0 + n\gamma_v$ linearly increasing with n, starting from a small value γ_0 for the 0−0 transition and increasing with a vibrational contribution γ_v, but this did not lead to significant improvement for the simultaneous fit of the absorption and HRS profiles. (ii) In the single-mode vibronic model, we only considered the two-level terms associated with each of the vibronic transitions contributing to the UV/vis absorption spectrum, neglecting the three-level diagrams in the hyperpolarizability that also involve the purely vibrational transitions in the ground or excited state that have for instance been found to be important in the modeling of two-photon absorption spectra.[62] This approximation is also applied in the more comprehensive model of Moran et al.[41] and was shown later to be adequate in the case of a donor−acceptor substituted polyene.[53] The diagrams with vibrational transitions in the electronic ground state lead to resonances in the far-IR region and they were in a number of cases shown to be dominant over the purely electronic contributions for the static limit of the NLO polarizabilities. Although they turn out to be important at all frequencies for the EO hyperpolarizability $\beta(-\omega;\omega,0)$, the effect in the optical frequency range on $\beta(-2\omega;\omega,\omega)$ of interest here was shown for several organic chromophores to be relatively small and monotonously decreasing with frequency.[37,63] We found that the introduction of such three-level type diagrams into the β expressions had no significant effect on the dispersion curve in the studied range (although the behavior in the far IR and the static limit can, of course, be very different). (iii) We also tried to take the higher energy electronic transition (absorption band at 330 nm, see Figure 4) into account, but it was found that the addition of neither two-level nor three-level diagrams had a significant influence on the shape of the low-energy resonance, although both can, of course, improve the description of the shorter wavelength resonance of β. This unexpected result can be attributed to the coherent addition of the extra term, causing little effect at frequencies where the first term is small.

Other approximations are harder to overcome: **(i)** In the vibrational model, $\Delta\mu$ is supposed to be the same for all of the vibrational sublevels. This may be inappropriate in the case of strong vibronic coupling which can be expected in these zwitterionic chromophores. For instance, in the BLA model,[25,26] or in the adiabatic D−A model proposed by Painelli,[32] the ground and excited electronic states vary strongly as a function of vibrational coordinate. It is very well possible that this variation of $\Delta\mu$ causes an additional shift of the β resonance relative to absorption, but unfortunately, it is not straightforward to include this effect in the model. (ii) Simultaneous coupling to several vibrational modes could be important, and this can be implemented in the approach of refs 41, 53, and 54, which involves a parallel fitting of the absorption spectra and the resonant (hyper-)Raman profiles of the system. It would certainly be of interest to apply this model to the present wavelength-dependent HRS data of PQDM in future work, but this requires the determination of many additional parameters.

The two vibronic models considered here represent in fact two opposite limiting cases of either an infinite number of vibronic lines (no inhomogeneous broadening) or only a single vibrational mode (combined with inhomogeneous broadening). The real situation would be in between both limiting cases. Indeed, also the comparison with experiment (Figure 5b) shows that both models deviate in opposite directions: the former predicts a β resonance profile that is slightly too broad and the latter a too narrow one. This indicates that a more adequate model of the vibrational mode structure, intermediate between the two vibronic models that were applied here, could lead to an even better description of the observed β dispersion.

Although the differences between the various models might seem relatively subtle, the β values extrapolated to the static limit are extremely different. The undamped TLM yields values varying widely in the range $\beta_0 = 29-686 \times 10^{-30}$ esu, calculated from the β values at 1300 and 1500 nm, respectively, or even 871×10^{-30} esu from the value measured at 780 nm close to the high-energy resonance. Based on the least resonant β value, at 1730 nm, $\beta_0 = 458 \times 10^{-30}$ esu is obtained. Fitting with the various models that include line broadening effects also leads to very different results. The models involving only homogeneous broadening mechanisms tend to yield relatively high β_0 values, especially the homogeneously damped TLM ($\beta_0 = 874 \times 10^{-30}$ esu) but also the purely homogeneous vibronic-like model ($\beta_0 = 514 \times 10^{-30}$ esu, and 526×10^{-30} esu for the

closely related absorption-based Kelley model). On the contrary, when inhomogeneous broadening is involved, this leads to lower β_0 values (for the inhomogeneously broadened TLM [$\beta_0 = 99 \times 10^{-30}$ esu] as well as for the single-mode vibronic model with small damping [$\beta_0 = 144 \times 10^{-30}$ esu]) because incoherent addition leads to relatively large contributions of the most resonant molecules in the inhomogeneous distribution. The amplitude fit parameters in the various models can also be related to $\Delta\mu$ values, which are found to scale to a very good approximation linearly with the corresponding β_0 values. Note that even the β_0 values from the two most realistic models are very different (144 and 514×10^{-30} esu), even though both are perfectly consistent with the experimental absorption spectrum and both give a reasonable description of β in the two-photon resonance region. As these models are two extreme limiting cases, these two values can be considered as lower and upper limits to the static electronic hyperpolarizability. If the β dispersion curves derived from these vibronic models (see Figure 5b) are scaled to fit the lowest-frequency data point only (which is lying just outside of the two-photon resonance region, see Figure 4), this narrows down the upper and lower bounds for the static electronic hyperpolarizability to $\beta_0 = 247 - 397 \times 10^{-30}$ esu.

Conclusions

The dispersion of the first hyperpolarizability β of the zwitterionic chromophore PQDM was determined experimentally by HRS measurements over a very wide wavelength range, covering the entire two-photon resonance with the ICT band and also showing a second resonance at higher energy. Thanks to the high sensitivity of the HRS-setup reliable calibration against the pure solvent could be used at all wavelengths and dependable β values were obtained even in the weak IR absorption bands of the solvent, as demonstrated by measurements in deuterated DMF. A pronounced red shift of the β dispersion resonance compared to the absorption maximum is observed, which is not explained by previously available models. The new models including purely inhomogeneous and/or vibronic broadening all lead to an appreciable red shift of 22 − 31 nm, approaching the experimental estimate of 33 nm (in SH wavelength) in the case of the simple vibronic model. The inhomogeneously broadened TLM yields a simple expression to estimate this red shift (eq 6). The best results for the description of the overall shape of the β resonance curve are obtained with the models in which mainly vibronic coupling is responsible for the observed absorption bandwidth. It is important to note that this is also the more physically realistic situation. We further stress the importance of describing the β dispersion using a model that is also consistent with the experimentally observed absorption spectrum, which is information that is readily and very accurately available for any compound. In general, models including more inhomogeneous broadening lead to a narrower β resonance peak (and smaller extrapolated β_0), whereas more homogeneous broadening (including damping and vibronic coupling) results in a broader resonance (and larger β_0). Results from two extreme limiting cases of vibronic models (infinite number of narrow vibronic lines vs a single mode with inhomogeneous broadening) suggest that an intermediate, more refined vibronic model (requiring more parameters) can give a very accurate description of the observed β dispersion. The present observations are also clearly demonstrating that one should be most careful in extrapolating experimental β values to the static limit within the currently available models, even when line-broadening mechanisms are included.

Acknowledgment. Financial support from the Fund for Scientific Research of Flanders (FWO − Vlaanderen, Belgium) in the group projects G.0041.01 and G.0129.07 is gratefully acknowledged. W.W. is a Postdoctoral Fellow of the FWO.

Supporting Information Available: Figure showing the effect of increasing homogeneous width on absorption and β dispersion within the single-mode vibronic model. This material is available free of charge via the Internet at http://pubs.acs.org.

References and Notes

(1) Prasad, P. N.; Williams, D. J., *Introduction to Nonlinear Optical Effects in Molecules and Polymers*; John Wiley and Sons: New York, 1991.
(2) Shi, Y. Q.; Lin, W. P.; Olson, D. J.; Bechtel, J. H.; Zhang, H.; Steier, W. H.; Zhang, C.; Dalton, L. R. *Appl. Phys. Lett.* **2000**, *77*, 1.
(3) Dalton, L.; Harper, A.; Ren, A.; Wang, F.; Todorova, G.; Chen, J.; Zhang, C.; Lee, M. *Ind. Eng. Chem. Res.* **1999**, *38*, 8.
(4) Chang, C. C.; Chen, C. P.; Chou, C. C.; Kuo, W. J.; Jeng, R. J. *J. Macromol. Sci.-Polym. Rev.* **2005**, *C45*, 125.
(5) Terhune, R. W.; Maker, P. D.; Savage, C. M. *Phys. Rev. Lett.* **1965**, *14*, 681.
(6) Clays, K.; Persoons, A. *Phys. Rev. Lett.* **1991**, *66*, 2980.
(7) Oudar, J. L.; Chemla, D. S. *J. Chem. Phys.* **1977**, *66*, 2664.
(8) Di Bella, S. *New J. Chem.* **2002**, *26*, 495.
(9) Uyeda, H. T.; Zhao, Y. X.; Wostyn, K.; Asselberghs, I.; Clays, K.; Persoons, A.; Therien, M. J. *J. Am. Chem. Soc.* **2002**, *124*, 13806.
(10) Dhenaut, C.; Ledoux, I.; Samuel, I. D. W.; Zyss, J.; Bourgault, M.; Lebozec, H. *Nature* **1995**, *374*, 339.
(11) Kaatz, P.; Shelton, D. P. *J. Chem. Phys.* **1996**, *105*, 3918.
(12) Ledoux, I.; Zyss, J. *Pure Appl. Opt.* **1996**, *5*, 603.
(13) Stadler, S.; Dietrich, R.; Bourhill, G.; Brauchle, C. *Opt. Lett.* **1996**, *21*, 251.
(14) Stadler, S.; Dietrich, R.; Bourhill, G.; Brauchle, C.; Pawlik, A.; Grahn, W. *Chem. Phys. Lett.* **1995**, *247*, 271.
(15) Woodford, J. N.; Wang, C. H.; Jen, A. K. Y. *Chem. Phys.* **2001**, *271*, 137.
(16) Pauley, M. A.; Wang, C. H. *Chem. Phys. Lett.* **1997**, *280*, 544.
(17) Le Bozec, H.; Le Bouder, T.; Maury, O.; Ledoux, I.; Zyss, J. *J. Opt. A* **2002**, *4*, S189.
(18) Hsu, C. C.; Liu, S.; Wang, C. C.; Wang, C. H. *J. Chem. Phys.* **2001**, *114*, 7103.
(19) Wang, C. H.; Lin, Y. C.; Tai, O. Y.; Jen, A. K. Y. *J. Chem. Phys.* **2003**, *119*, 6237.
(20) Hung, S. T.; Wang, C. H.; Kelley, A. M. *J. Chem. Phys.* **2005**, *123*, 144503.
(21) Tai, O. Y. H.; Wang, C. H.; Ma, H.; Jen, A. K. Y. *J. Chem. Phys.* **2004**, *121*, 6086.
(22) Ashwell, G. J. *Thin Solid Films* **1990**, *186*, 155.
(23) Boldt, P.; Bourhill, G.; Brauchle, C.; Jim, Y.; Kammler, R.; Muller, C.; Rase, J.; Wichern, J. *Chem. Comm.* **1996**, 793.
(24) Szablewski, M.; Thomas, P. R.; Thornton, A.; Bloor, D.; Cross, G. H.; Cole, J. M.; Howard, J. A. K.; Malagoli, M.; Meyers, F.; Bredas, J. L.; Wenseleers, W.; Goovaerts, E. *J. Am. Chem. Soc.* **1997**, *119*, 3144.
(25) Marder, S. R.; Perry, J. W.; Bourhill, G.; Gorman, C. B.; Tiemann, B. G.; Mansour, K. *Science* **1993**, *261*, 186.
(26) Marder, S. R.; Beratan, D. N.; Cheng, L. T. *Science* **1991**, *252*, 103.
(27) Beaudin, A. M. R.; Song, N. H.; Bai, Y. W.; Men, L. Q.; Gao, H. P.; Wang, Z. Y.; Szablewski, M.; Cross, G.; Wenseleers, W.; Campo, J.; Goovaerts, E. *Chem. Mater.* **2006**, *18*, 1079.
(28) Song, N. H.; Men, L. Q.; Gao, J. P.; Bai, Y. W.; Beaudin, A. M. R.; Yu, G. M.; Wang, Z. Y. *Chem. Mater.* **2004**, *16*, 3708.
(29) Orr, B. J.; Ward, J. F. *Mol. Phys.* **1971**, *20*, 513.
(30) Otomo, A.; Jager, M.; Stegeman, G. I.; Flipse, M. C.; Diemeer, M. *Appl. Phys. Lett.* **1996**, *69*, 1991.
(31) Otomo, A.; Stegeman, G. I.; Flipse, M. C.; Diemeer, M. B. J.; Horsthuis, W. H. G.; Mohlmann, G. R. *J. Opt. Soc. Am. B* **1998**, *15*, 759.
(32) Painelli, A. *Chem. Phys. Lett.* **1998**, *285*, 352.
(33) Painelli, A. *Synth. Met.* **1999**, *101*, 218.
(34) Bishop, D. M.; Kirtman, B. *J. Chem. Phys.* **1991**, *95*, 2646.
(35) Bishop, D. M.; Champagne, B.; Kirtman, B. *J. Chem. Phys.* **1998**, *109*, 9987.
(36) Bishop, D. M.; Norman, P. In *Handbook of Advanced Electronic and Photonic Materials and Devices*; Nalwa, H. S., Ed.; Academic Press: New York, 2001; Vol. 9, Chapter 1.
(37) Champagne, B.; Kirtman, B. In *Handbook of Advanced Electronic and Photonic Materials and Devices*; Nalwa, H. S., Ed.; Academic Press: New York, 2001; Vol. 9,, Chapter 2.
(38) Zuliani, P.; Del Zoppo, M.; Castiglioni, C.; Zerbi, G.; Andraud, C.; Brotin, T.; Collet, A. *J. Phys. Chem.* **1995**, *99*, 16242.

(39) Castiglioni, C.; Del Zoppo, M.; Zerbi, G. *Phys. Rev. B* **1996**, *53*, 13319.

(40) Castiglioni, C.; Del Zoppo, M.; Zuliani, P.; Zerbi, G. *Synth. Met.* **1995**, *74*, 171.

(41) Moran, A. M.; Egolf, D. S.; Blanchard-Desce, M.; Kelley, A. M. *J. Chem. Phys.* **2002**, *116*, 2542.

(42) Shoute, L. C. T.; Helburn, R.; Kelley, A. M. *J. Phys. Chem. A* **2007**, *111*, 1251.

(43) Kelley, A. M. *J. Opt. Soc. Am. B* **2002**, *19*, 1890.

(44) Flipse, M. C.; Dejonge, R.; Woudenberg, R. H.; Marsman, A. W.; Vanwalree, C. A.; Jenneskens, L. W. *Chem. Phys. Lett.* **1995**, *245*, 297.

(45) Goovaerts, E.; Wenseleers, W.; Garcia, M. H.; Cross, G. H. In *Handbook of Advanced Electronic and Photonic Materials and Devices*; Nalwa, H. S., Ed.; Academic Press: New York, 2001; Vol. 9, Chapter 3.

(46) Kajzar, F.; Ledoux, I.; Zyss, J. *Phys. Rev. A* **1987**, *36*, 2210.

(47) Kaatz, P.; Donley, E. A.; Shelton, D. P. *J. Chem. Phys.* **1998**, *108*, 849.

(48) Berkovic, G.; Meshulam, G.; Kotler, Z. *J. Chem. Phys.* **2000**, *112*, 3997.

(49) Oudar, J. L. *J. Chem. Phys.* **1977**, *67*, 446.

(50) Wang, C. H. *J. Chem. Phys.* **2000**, *112*, 1917.

(51) Krishnan, A.; Pal, S. K.; Nandakumar, P.; Samuelson, A. G.; Das, P. K. *Chem. Phys.* **2001**, *265*, 313.

(52) Wang, C. H.; Woodford, J. N.; Zhang, C.; Dalton, L. R. *J. Appl. Phys.* **2001**, *89*, 4209.

(53) Shoute, L. C. T.; Blanchard-Desce, M.; Kelley, A. M. *J. Phys. Chem. A* **2005**, *109*, 10503.

(54) Shoute, L. C. T.; Bartholomew, G. P.; Bazan, G. C.; Kelley, A. M. *J. Chem. Phys.* **2005**, *122*, 184508.

(55) Shoute, L. C. T.; Woo, H. Y.; Vak, D.; Bazan, G. C.; Kelley, A. M. *J. Chem. Phys.* **2006**, *125*, 054506.

(56) Fowler, W. B., Ed.; *Physics of Color Centers*; Academic: New York, 1968.

(57) Wang, C. H.; Woodford, J. N.; Jen, A. K. Y. *Chem. Phys.* **2000**, *262*, 475.

(58) Robalo, M. P.; Teixeira, A. P. S.; Garcia, M. H.; da Piedade, M. F. M.; Duarte, M. T.; Dias, A. R.; Campo, J.; Wenseleers, W.; Goovaerts, E. *Eur. J. Inorg. Chem.* **2006**, 2175.

(59) Woodford, J. N.; Wang, C. H.; Asato, A. E.; Liu, R. S. H. *J. Chem. Phys.* **1999**, *111*, 4621.

(60) A small change of the value of ω_{eg} in eq 9 is expected to have no significant effect on the two-photon resonance because ω_{eg} only occurs in the first term and in the prefactor, which are both only slowly varying at that resonance. Indeed, the use of the value of $\lambda_{eg} = 638$ nm instead of $\lambda_{max} = 647$ nm only results in a negligible additional red shift ($\sim$0.3 nm in SH wavelength) of the two-photon resonance (whereas the undamped one-photon resonance is of course blue shifted).

(61) Myers, A. B. *Annu. Rev. Phys. Chem.* **1998**, *49*, 267.

(62) Painelli, A.; Del Freo, L.; Terenziani, F. *Chem. Phys. Lett.* **2001**, *346*, 470.

(63) Bishop, D. M.; Gu, F. L.; Cybulski S. M. *J. Chem. Phys.* **1998**, *109*, 8407.